Baidya, Avijit; Yatheendran, Anagha; Ahuja, Tripti; Sudhakar, Chennu; Das, Sarit Kumar; Ras, Robin H.A.; Pradeep, Thalappil

Waterborne Fluorine-Free Superhydrophobic Surfaces Exhibiting Simultaneous CO_2 and Humidity Sorption

Published in:
Advanced Materials Interfaces

DOI:
10.1002/admi.201901013

Published: 01/01/2019

Document Version
Other version

Supporting Information

Waterborne Fluorine-Free Superhydrophobic Surfaces Exhibiting Simultaneous CO_2 and Humidity Sorption

*Avijit Baidya[a,b,c], Anagha Yatheendran[a], Tripti Ahuja[a], Chennu Sudhakar[a], Sarit Kumar Das[c], Robin H.A. Ras[b,d], Thalappil Pradeep[a,]**

[a]DST Unit of Nanoscience, Thematic Unit of Excellence, Department of Chemistry, Indian Institute of Technology Madras, Chennai, India, E-mail: pradeep@iitm.ac.in

[b]Department of Applied Physics, Aalto University School of Science, Puumiehenkuja 2, 02150 Espoo, Finland

[c]Department of Mechanical Engineering, Indian Institute of Technology Madras, Chennai 600036, India

[d]Department of Bioproducts and Biosystems, Aalto University School of Chemical Engineering, Kemistintie 1, 02150 Espoo, Finland

Table of contents

	adhesion test over sand paper abraded surface	
S11	Oil-wash experiment	8
S12	Change in wetting property of the coated surfaces upon immersion inside various organic solvents for 50 h. Static CA and CAH of water droplet was measured after taking the surface out from the solvent in a regular time interval of 5 h	8
S13	CA measurements with acidic (pH=1) and basic (pH=14) water droplet	9
S14	VADTs with acidic (pH=1) and basic (pH=14) water droplet	9
S15	(a) CA measurements over 200, 225, 250 ºC temperature treated surface. (b) VADTs over 250 ºC temperature treated surface	10
S16	Moisture adsorption studies with filter paper and native clay (NC)	10
S17	Effect of temperature on moisture adsorption	11
S18	Static water contact angle over humidity adsorbed superhydrophobic surface.	11
S19	Schematic presentation of fabrication process	12
S20	Effect of drying temperature on non-wetting property of the material	12
S21	Stability of the chemical attachments between AS and OS with clay particles	12

Video No.	Description
V1	Droplet drag test (DDT) over superhydrophobic surface
V2	Verticle droplet adhesion test (VDAT) over superhydrophobic surface
V3	Bouncing of water droplet over coated filter paper
V4	Droplet drag test (DDT) over finger-wiped superhydrophobic surface
V5	Vertical droplet adhesion test (VDAT) over sand paper abraded superhydrophobic surface
V6	Self-cleaning property and movement of water droplets over THF-washed superhydrophobic surface
V7	Vertical droplet test (VDAT) over high temp treated superhydrophobic surface
V8	Droplet drag test (DDT) and vertical droplet adhesion test (VDAT) over moisture saturated superhydrophobic surface

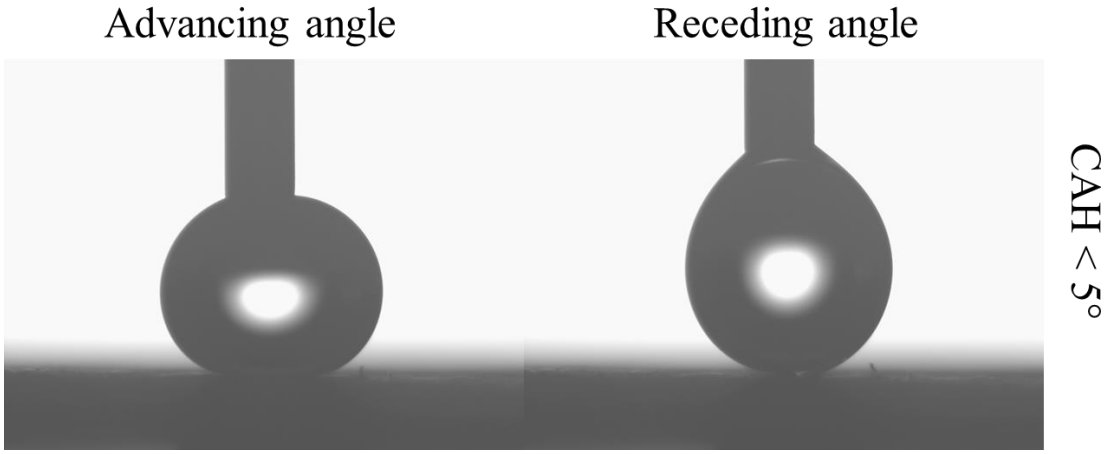

Figure S1. Advancing angle (170°), receding angle (167°) and the difference of these two, contact angle hysteresis (CAH) over coated surface.

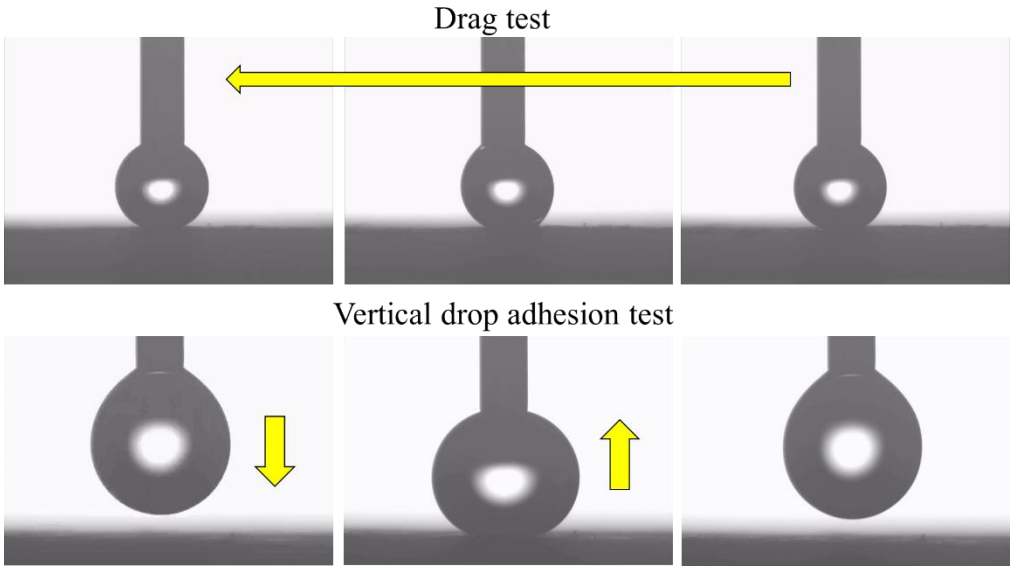

Figure S2. Drag test and vertical drop adhesion test over superhydrophobic surface. Arrows represent the directions of droplet movement.

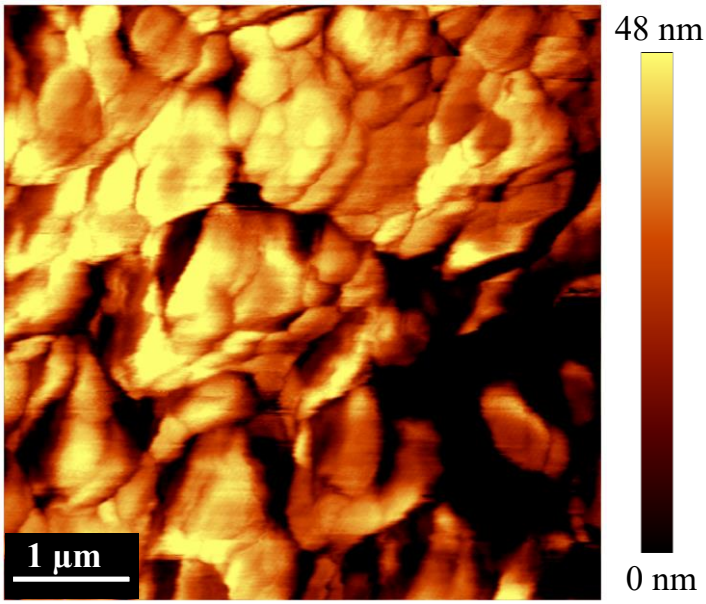

Figure S3. AFM image of unmodified clay coated glass surface.

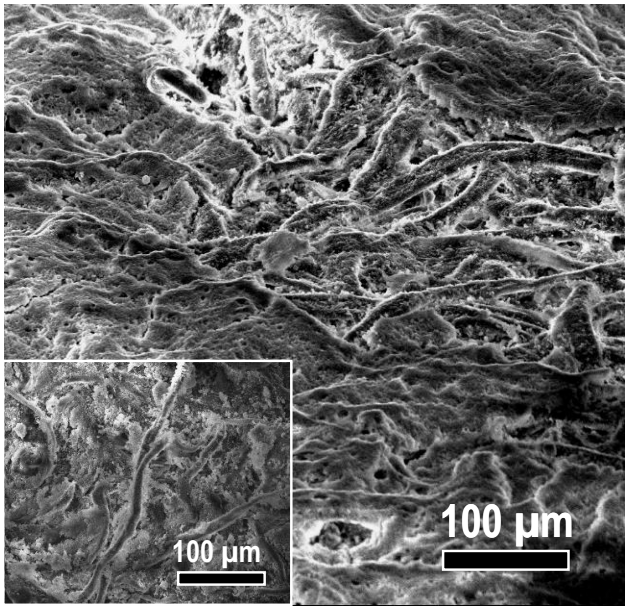

Figure S4. SEM image of modified clay coated filter paper (tilt angle 45°). (Inset) Perpendicular view.

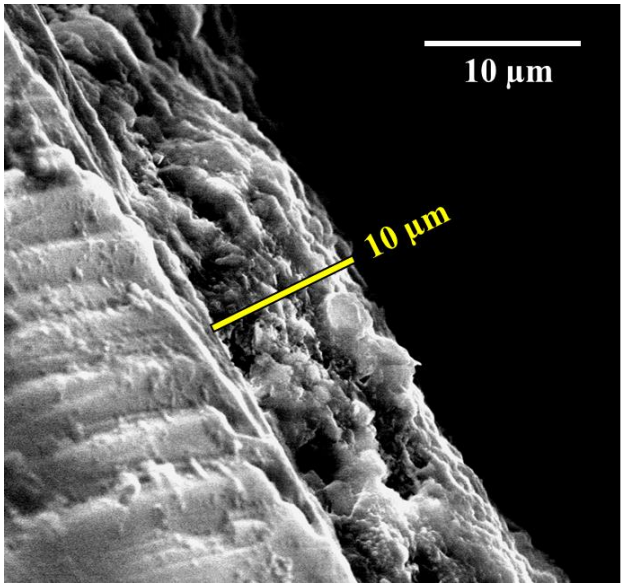

Figure S5. Cross-sectional SEM image shows the thickness of the coating.

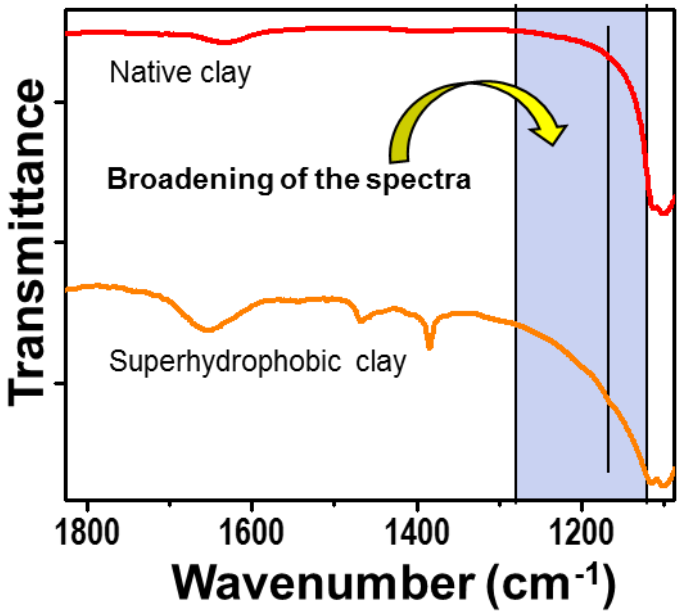

Figure S6. Expanded IR spectra of superhydrophobic clay and native clay. Hump at 1170 cm^{-1} and broading of the spectrum for superhydrophobic clay (marked in black line and blue shade) corresponds to the C-N stratching, coming from the incorporated amine functionality.

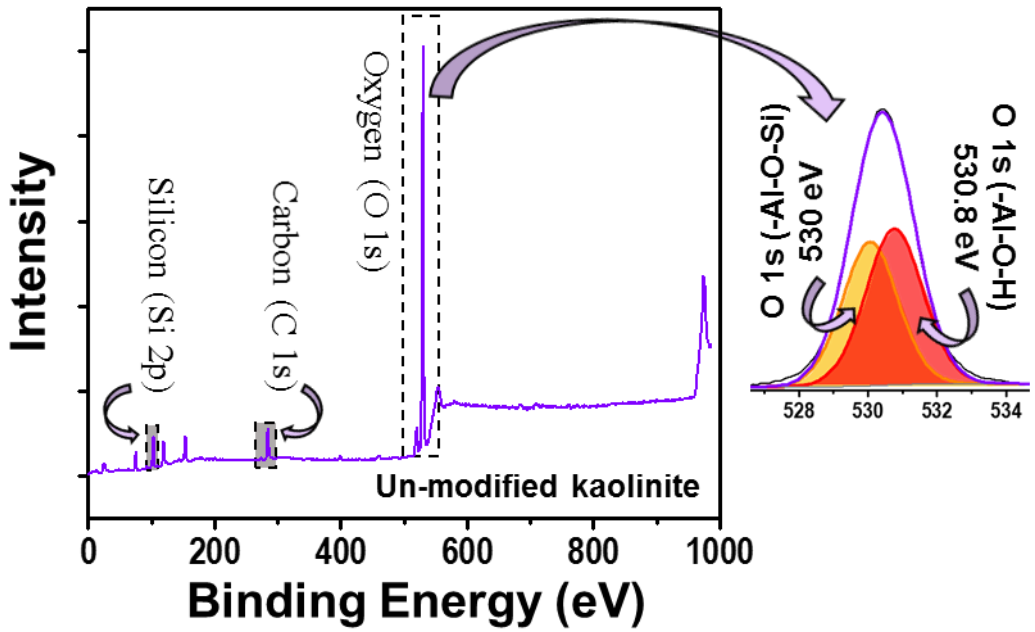

Figure S7. Survey spectrum and deconvoluted XPS spectrum in the O1s region showing the relative concentration of Al-O-H and Al-O-Si linkage over native clay coated surface.

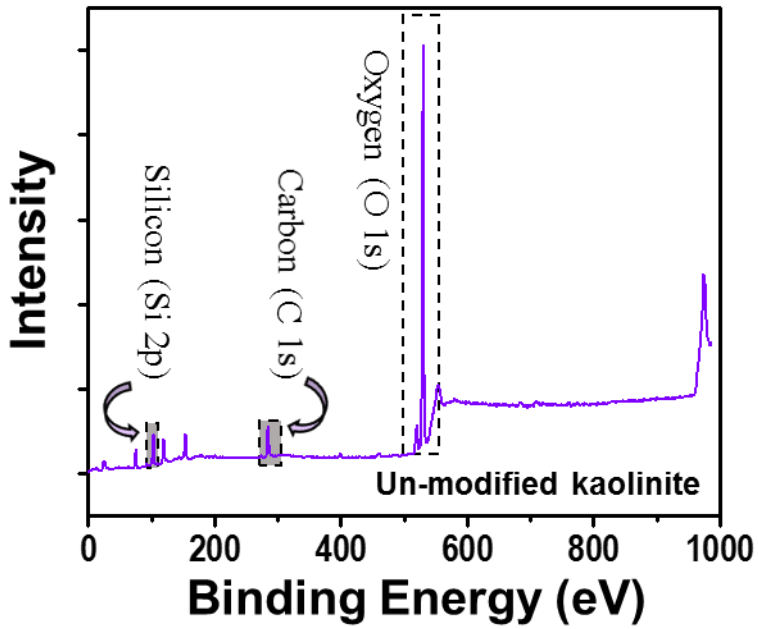

Figure S8. XPS survey spectrum of native clay. Peak at 285 eV corresponds to carbon, mostly comes from the organic species.

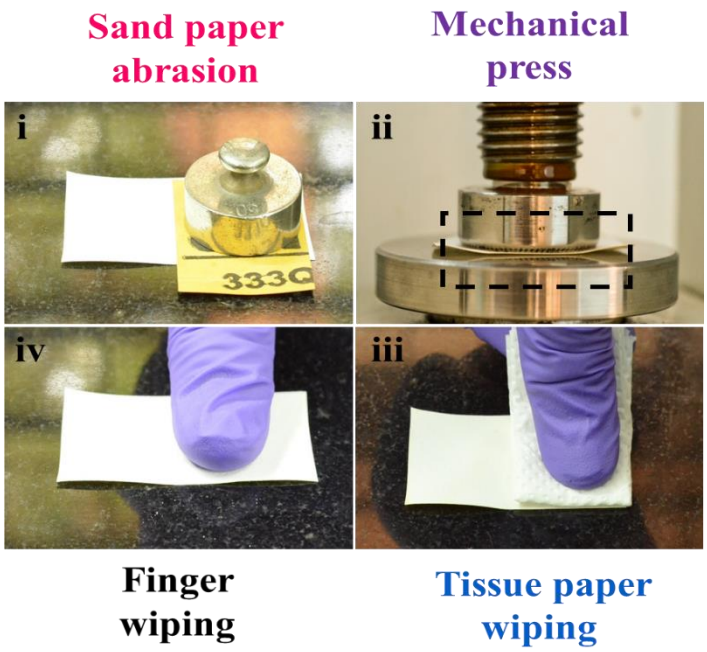

Figure S9. Image of various mechanical test. i) Sand paper abrasion, ii) mechanical pressing, iii) tissue paper wiping and iv) finger wiping.

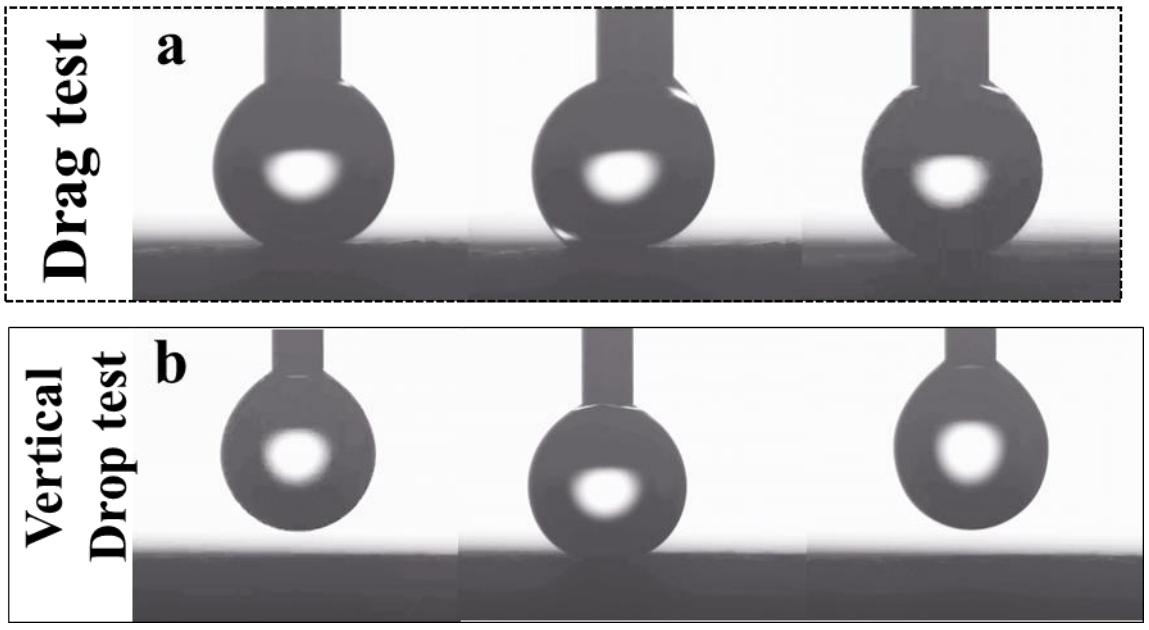

Figure S10. Image of (**a**) droplet drag test over finger wiped surface and (**b**) vertical droplet adhesion test over sand paper abraded surface.

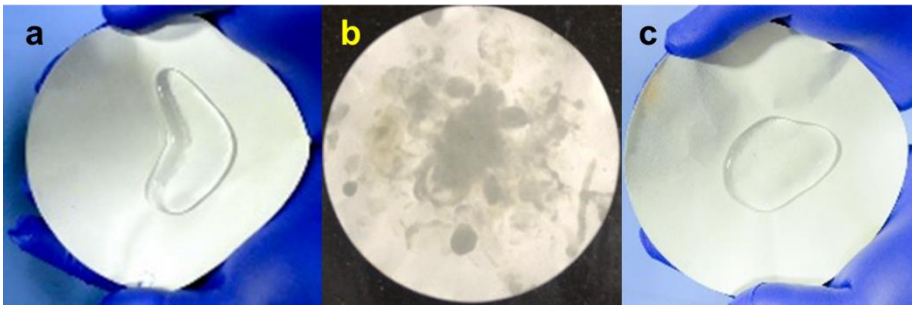

Figure S11. Oil-wash experiment. Image of (**a**) water over untreated superhydrophobic surface, (**b**) adsorbed oil over the superhydrophobic surface and (**c**) water over oil-washed superhydrophobic surface.

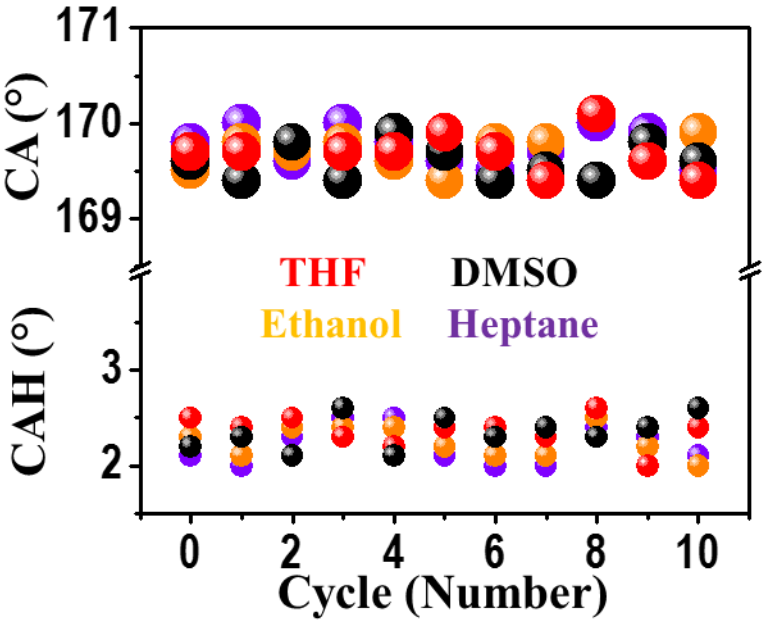

Figure S12. Change in wetting property of the coated surfaces upon immersion inside various organic solvents for 50 h. Static CA and CAH of water droplet was measured after taking the surface out from the solvent in a regular time interval of 5 h.

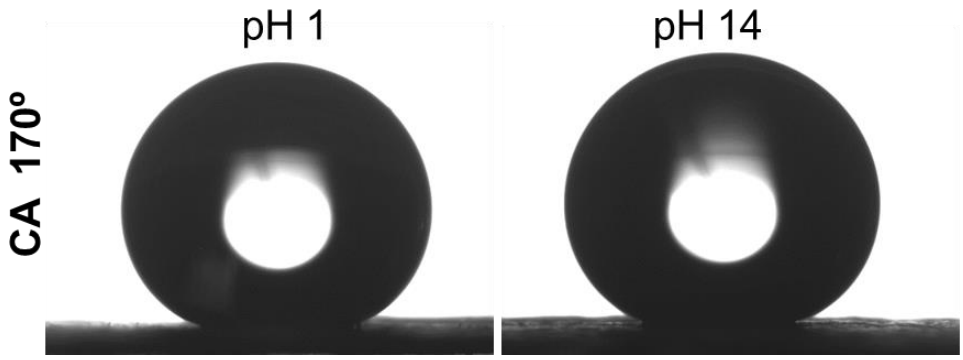

Figure S13. CA measurements with acidic (pH=1) and basic (pH=14) water droplets.

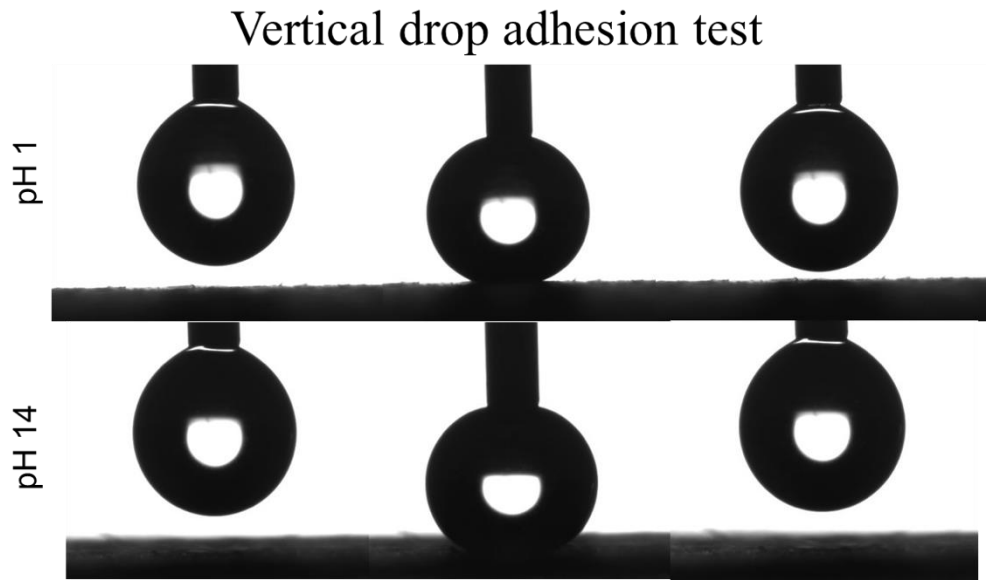

Figure S14. VDATs measurements with acidic (pH=1) and basic (pH=14) water droplets.

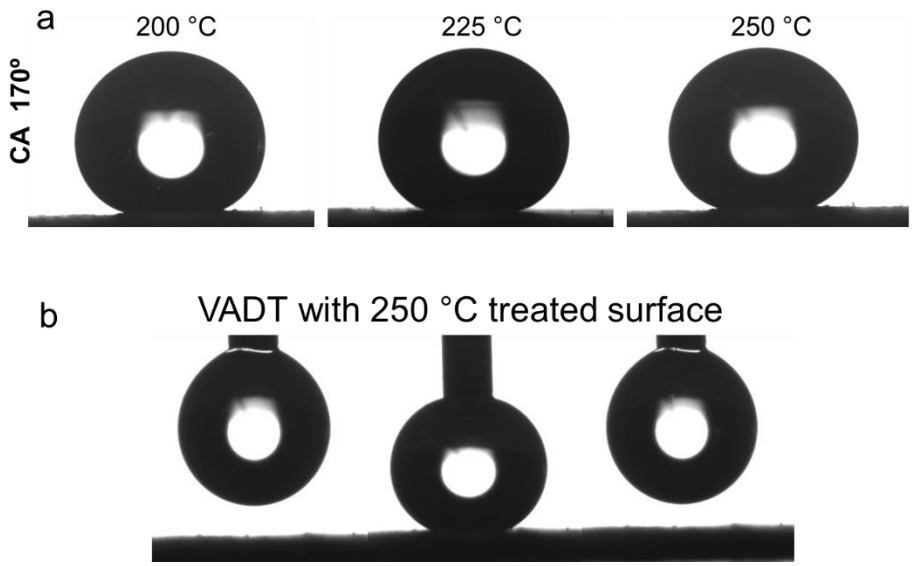

Figure S15. (a) CA measurements over 200, 225, 250 ºC temperature treated surface. (b) VADTs over 250 ºC temperature treated surface

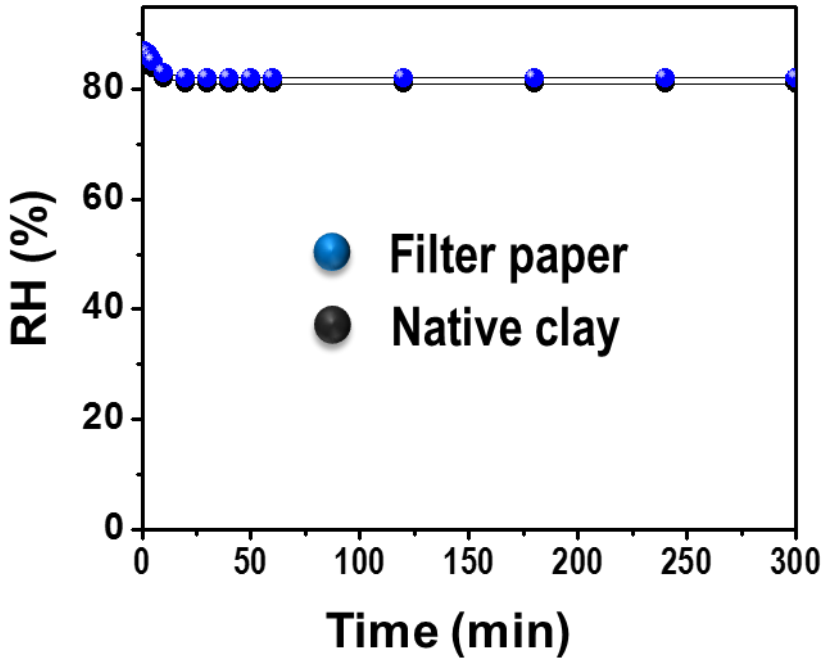

Figure S16. Moisture adsorption control study with filter paper and native clay.

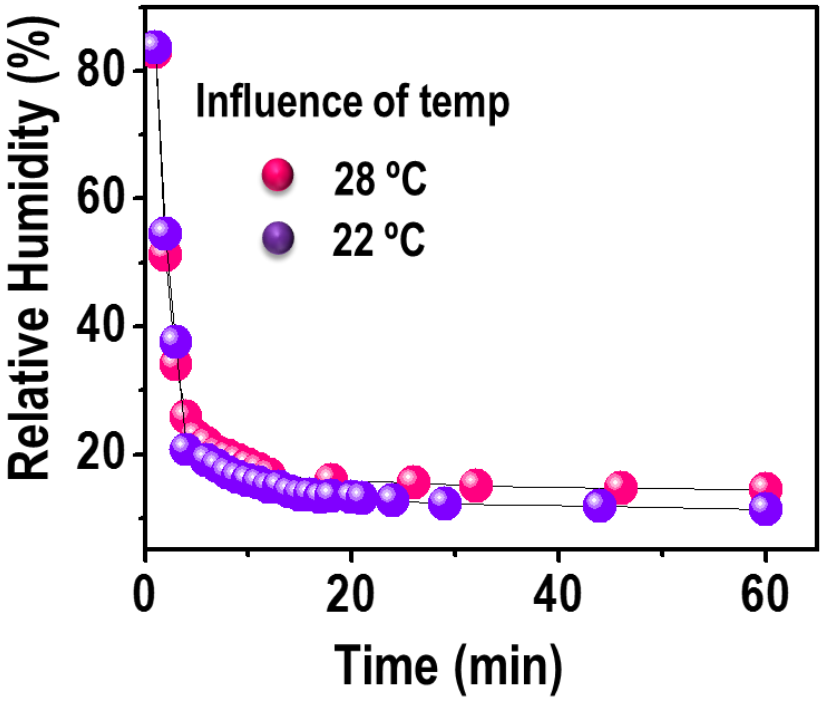

Figure S17. Effect of temperature on moisture adsorption

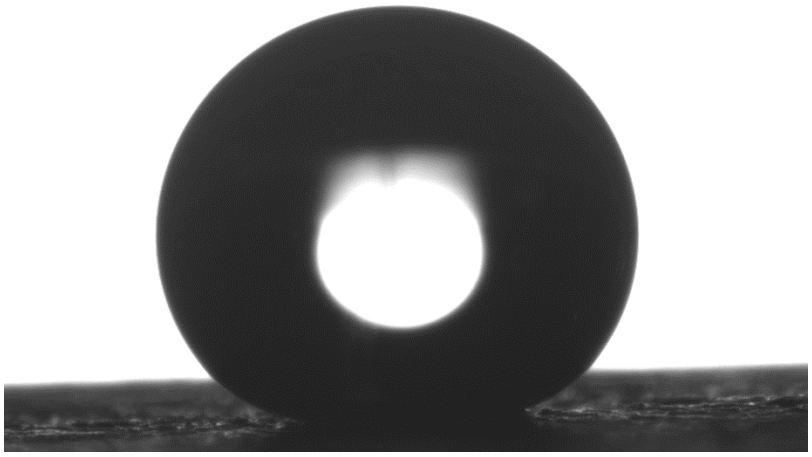

Figure S18. Static water contact angle (170°) over moisture adsorbed superhydrophobic surface.

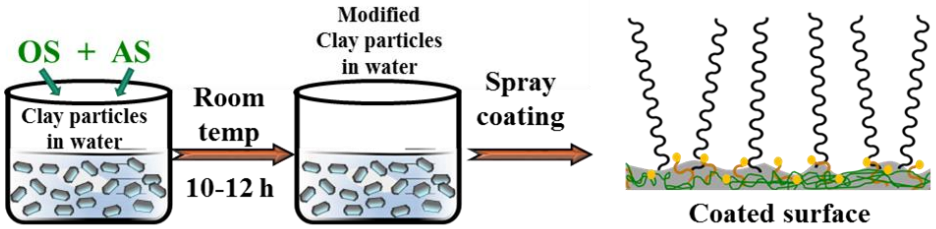

Figure S19. Schematic presentation of fabrication process.

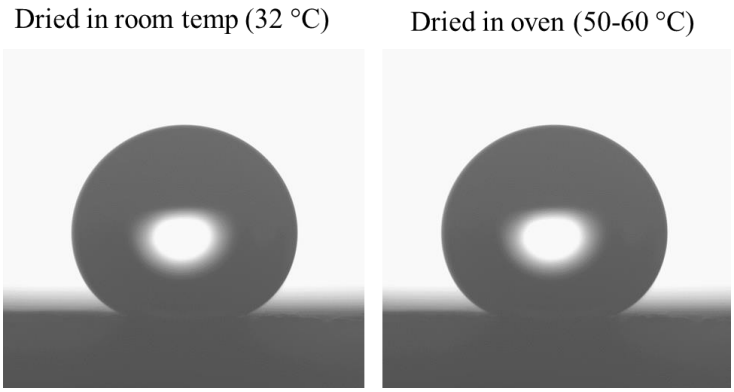

Figure S20. Effect of drying temperature on non-wetting property of the material. In both the cases static contact angle of water droplet was 170°.

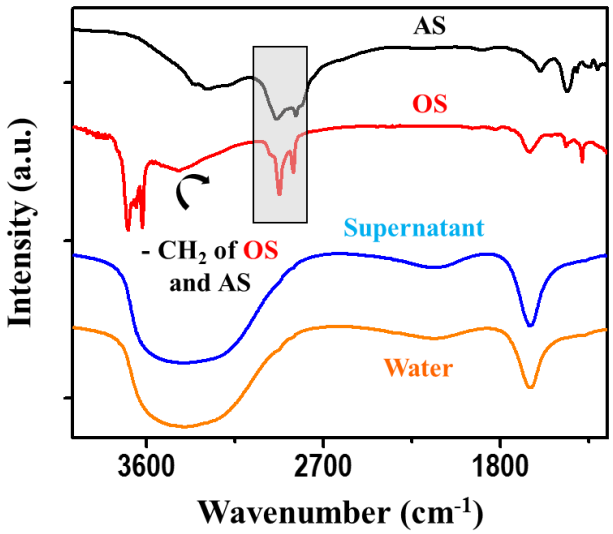

Figure S21. Stability of the chemical attachments between AS and OS with clay particles. IR spectra of supernatant, AS, OS, and water. IR spectrum of supernatant (blue) does not contain any characteristic peak of AS (black) and OS (red). It is similar to pure water (orange).